JKPK (Jurnal Kimia dan Pendidikan Kimia), Vol. 10, No. 3., 2025 Hal. 527-543
Chemistry Education Study Program Universitas Sebelas Maret ISSN 2503-4146
http://jurnal.uns.ac.id/jkpk ISSN 2503-4154 (online)

Green Synthesis of Silver Nanoparticles using Lemongrass Leaf (*Cymbopogon citratus*) Extract as a Reductant for Novel Colorimetric Mercury(II) Detection

Yussi Pratiwi[1]*, Yogi Febrian[1], Listya Eka Anggraini[2], Harfi Amania Khansa[1], and Rizkia Chandra Widianti[1]

[1] *Department of Chemistry, Faculty Mathematics and Sciences, Universitas Negeri Jakarta, Rawamangun, East Jakarta, Indonesia*

[2] *Department of Chemistry, King Fahd University of Petroleum and Minerals (KFUPM), Dhahran 31261, Saudi Arabia*

ABSTRACT

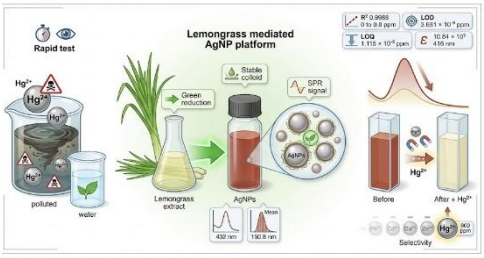

Mercury(II) contamination in water poses serious risks to human health, requiring rapid detection. This study develops a fast colorimetric sensor based on silver nanoparticles (AgNPs) synthesized using lemongrass (Cymbopogon citratus) leaf extract as a green reducing agent. Synthesis conditions were optimized, the AgNPs were characterized, and analytical performance was validated using standard parameters. Sensor responses were monitored by UV Vis spectroscopy through changes in the surface plasmon resonance (SPR) band and quantified from absorbance variations. The optimum synthesis produced a reddish brown AgNP colloid at 45 minutes, 3 mM AgNO3, and 10% lemongrass extract. The nanoparticles showed a maximum absorption at 432 nm and an average size of 150.8 nm. Validation results indicate excellent selectivity for Hg^{2+} and a pronounced change in the overall SPR signal at 600 ppm Hg^{2+}. The method was linear over 0 to 0.8 ppm Hg^{2+} with R^2 = 0.9988 (y = 0.04x + 0.0722). The limits of detection and quantification were 3.681 × 10^{-9} ppm and 1.115 × 10^{-8} ppm, respectively. Molar absorptivity reached 10.84 × 10^3 L mol^{-1} cm^{-1} at 416 nm. These results demonstrate that lemongrass mediated AgNPs provide a simple, rapid, and sensitive platform for mercury detection in water.

Keywords: *Colorimetric Sensors; Mercury Detection; Lemongrass; Silver Nanoparticle.*

**Corresponding Author: yussipratiwi@unj.ac.id*

How to cite: Y. Pratiwi, Y. Febrian, L. E. Anggraini, H. A. Khansa, and R. C. Widianti, "Green synthesis of silver nanoparticles using lemongrass leaf (*Cymbopogon citratus*) extract as a reductant for novel colorimetric mercury(II) detection," *JKPK (Jurnal Kimia dan Pendidikan Kimia)*, vol. 10, no. 3, pp. 527-543, 2025. [Online]. Available: https://doi.org/10.20961/jkpk.v10i3.109804

Received: *2025-10-11* ***Accepted:*** *2025-12-12* ***Published:*** *2025-12-31*

INTRODUCTION

Industrial activities is a major contributor to environmental pollution, especially waters in the form of heavy metal pollution with high toxicity such as mercury (Hg), Cadmium (Cd,), lead (Pb) which can affect water quality. Mercury is a highly toxic heavy metal because it is a neurotoxic to living organisms and humans. Moreover, mercury is difficult to decompose if it enters waterways. It is not only concentrated in water, but also settles in sediments. The Indonesian Ministry of Environment and Forestry, in Government Regulation Number 22 of 2021, sets the limit for mercury content in water at 0.002 ppm [1]. One of the rivers in Indonesia, the Ciujung River in Banten, has a

mercury concentration of around 0.7 ppm[2]. Thus, a detection method is required to confirm the presence of mercury in water, considering its potential hazards to human health.

Heavy metals can be analyzed using techniques such as Atomic Absorption Spectrophotometer (AAS) and Inductively Coupled Plasma - Mass Spectrometry (ICP-MS). However, these methods often involve complex instrumentation, high operational costs, and lengthy analysis times. Therefore, the development of more efficient detection methods for mercury in water is essential. One promising approach involves the use of silver nanoparticles (AgNPs) as colorimetric sensors, offering advantages such as rapid visual detection and reduced costs [3], [4]. AgNPs for heavy metal detection have been widely used. As [5] has synthesized AgNPs as Al^{3+} sensors, then [6] has synthesized AgNPs as Cu^{2+} sensors. In recent years, several AgNPs developments have been widely studied [7]. In general, nanoparticle synthesis can be done using top-down methods (physics) and bottom-up methods (chemistry).

Many harmless and biocompatible synthesis methods have been developed, particularly the green chemistry approaches, which emphasize sustainability in nanoparticle production [8]. Nanoparticle synthesis using the green chemistry method is a synthesis method that uses plant extracts as reducing agents from precursor metals, the green chemistry method has a shorter reaction time than physical and chemical methods. The use of plants in nanoparticle biosynthesis cannot be separated from the content of secondary metabolite compounds that are antioxidants such as flavonoids, alkaloids, phenols, tannins, and terpenoids.

These antioxidants can be an environmentally friendly alternative (green chemistry) for nanoparticle production because they can reduce the use of harmful chemicals, including the waste produced [9]. There have been many uses of natural antioxidants in plant extracts to synthesize AgNPs, such as Tectona grandis extract to produce AgNPs nanoparticles with a particle size of 10-30 nm [10]. Based on research conducted by [11], it shows that *Cymbopogon citratus* leaves contain a number of phytochemical compounds such as flavonoids, tannins, terpenoids and alkaloids. This plant is widely found throughout Indonesia, and the review findings indicate that AgNPs synthesized using this plant exhibit a uniform spherical shape and are free from aggregation, unlike those synthesized from various other plant extracts [12], [13].

In this study, *Cymbopogon citratus* leaves were used as a reducing agent and capping agent for AgNPs because it is known that *Cymbopogon citratus* leaves have high levels of antioxidant secondary metabolites [14]. Method validation is crucial for ensuring the reliability of AgNs as colorimetric sensor. Validation of analytical methods involves evaluating parameters through laboratory experiments to ensure that they meet the requirements for their use. Method validation is performed to ensure that the analysis method is accurate, specific, reproducible, and robust against the spectrum being analyzed. Some of the parameters evaluated in method validation include selectivity,

linearity, sensitivity, LOD, and LOQ. Based on the description above, this study focuses on synthesizing AgNPs using lemongrass leaf extract as a reducing agent for mercury(II) colorimetric detection, and also validating methods that include selectivity, sensitivity, linearity as well as LOD and LOQ.

METHODS

1. Materials and Instruments

The tools and materials used in this study were UV-Vis Spectrophotometer (UV Mini – 1240 Shimadzu), GC-MS (Agilent Technologies 7890), Particle Size Analyzer (Horiba Scientific SZ 100z), Fourier Transform Infra-Red (Alpha II Compact FT-IR Spectrometer), oven, analytical balance, stirring rod, pH specialized indicator (pH range 1-14), hot plate, magnetic stirrer, micropipette scale 100 − 1000 µL, petri cups, hair dryers, statives and clamps, vacuum pumps, blenders, separation funnels, glass funnels, spray bottles, bulbs, and glassware. Local lemongrass leaves (*Cymbopogon citratus*) obtained from the market around Mampang Prapatan. Analytical grade reagents such as $AgNO_3$, H_2SO_4 (96%), ethanol 96%, concentrated HCl, NaOH, Magnesium Chloride Anhydrate, Mercury(II) Nitrate Monohydrate, Aluminum Chloride, Cadmium Sulfate Octahydrate, Copper (II) Chloride Dihydrate, Lead (II) Nitrate, Manganese Sulfate Monohydrate, Zinc Chloride, and Potassium Iodide was procured from Merck. Another materials including aquadest, Whatmann filter paper No. 42, aluminum foil, and cling wrap were used in this experiment.

2. Preparation of Lemongrass Leaf Extract

Kitchen lemongrass leaves were washed several times with an aquadest to remove impurities, then dried at room temperature of 25°C for about 3 days, and then ground until it becomes a fine homogeneous powder (approximately 40-60 mesh). Then 847.7 g of dried lemongrass leaves were added to 5395 mL of 95% ethanol which has been distilled in a 10 L container then static maceration was carried out for 3x24 hours. The mixed solution that had been completed was then filtered using Whatmann filter paper No. 42 to obtain a solution of lemongrass leaf extract (ex-sol). Then the filtering results were stored in 1000 mL beaker glass at room temperature 25°C for 3x24 hours before further use. This ex-sol is the result of the extraction of ethanol fractions.

3. Ethanol Extract Fractionation

The results of the ethanol extract that have been stored are then extracted from the liquid using a separate funnel. Ethanol extracts were fractionated with n-hexane solvent (96%) analytical grade with a volume ratio (v/v) of 1:2. 300 mL of ethanol fraction was taken and 600 mL of n-hexane was added to the separation funnel and cornered. The result of the separation of the n-hexane fraction was discarded because all the secondary metabolites needed are in the ethanol fraction, whereas in n-hexane only the matrix is not needed, and then the ethanol fraction was stored in a container. This fractionation was repeated 3 times. The fractionated ethanol extract was vaporized with a rotatory evaporation until a thick

ethanol extract is obtained. Ethanol thick extract was added with aquadest solvent with a ratio (v/v) of 1:4. The ethanol extract that had been added aquadest is put into a separation funnel and fractionated with ethyl acetate solvent with a ratio (v/v) of 1:2. The results of 33 fractionations were obtained from liquid ethyl acetate extract and stored in a dark container at room temperature and then continued at the synthesis stage as a bioreductors.

4. Characterization of Lemongrass Leaf Extract Using Gas Chromatography Mass Spectrophotometry (GC-MS)

GC MS analysis was conducted to determine the percentage of organic compound components contained in the fractionated extract, the GC-MS instrument was used. This is done as a method to determine compounds that play an important role in the synthesis process of AgNPs as bioreductors. In the characterization of lemongrass leaf extract in the form of liquid, was injected as 5 µL. The standard setting of the device is set with a 99% Helium eluent gas specification with a flow rate of 1.2 mL/min. The specification of the column used is the HP Ultra 2. Capillary Column with a Length of 30 m × 0.20 (mm) I.D × 0.11 (µm) Thickness Film with an electron energy of 70 eV. Temperature 230°C (detector), 250°C (injector), 280°C (interphase). The column temperature is maintained at 80°C in 0 minutes and increased by 3°C/min to 150°C within 1 minute, and then increased by 20°C/min to 280°C within 26 minutes. The separation ratio used is 8 : 1.

5. Synthesis of Nanoparticles

A systematic optimization study was conducted to determine the ideal conditions for the synthesis of AgNPs. The variables tested including reaction time (0,15,30,45,60 minutes), lemongrass leaf extract concentration (5,7,10,12,5 and 15% from 15.7% initial extract concentration), and $AgNO_3$ concentration (1,2,3,4,5 mM) with total volume with a total reaction volume of 40 ml. The mixture is stirred using a magnetic stirrer at 800 RPM and placed on a hot plate (50-60℃) with pH 10 using NaOH. The mixed solution was left to stand depending on the chosen reaction time and until the color changes from yellow to dark brown. Changes in absorption intensity that occur during the formation of AgNPs were also observed with a spectrophotometer (Shimadzu UV-Vis Spectrophotometer) in the range of 300-600 nm.

6. Stabilization of Silver Nanoparticles

The results of colloidal AgNPs formed with their optimal state were observed and measured until the 30^{th} day. This was done to test the stability of the nanoparticles based on the change in maximum wavelength and absorption using a UV-Vis spectrophotometer.

7. Characterization of Ethyl Acetate Extracts and Nanoparticles

Fourier transform infrared (FTIR) spectroscopy was performed to identify functional groups present in the bioreductor extract and in the synthesized nanoparticles. Capping agent that can undergo changes in the functional group which will later be compared with the results of the synthesis of AgNPs. The result of fractionation of ethyl

acetate extract and colloidal nanoparticles that have been formed under optimal conditions is dried for up to 18 hours in an oven with a temperature of 60°C. Ethyl acetate fractions and nanoparticles that have dried were tested with FTIR with 32 scans, resoution of 4 cm^{-1} and spectral range of 4000-400 cm^{-1}.

Particle Size Analyzer (PSA) measurements were conducted to determine particle size distribution using a Horiba SZ 100 instrument.. Analysis parameters were set at 25°C with viscosity of 0.8872 cP and refractive index of 1.330, corresponding to water at 25°C. A measurement angle of 173° was applied, with 3 to 5 runs per sample and a duration of 10 to 20 seconds per run. Particle size distribution data were considered to support selection of the nanoparticle system for potential application as a colorimetric sensor.

The formation of AgNPs solutions in the form of colloids (collAgNPs) was determined using a UV-Vis spectrophotometer (Shimadzu UV-Vis Spectrophotometer) in the wavelength range of 300– 600 nm. Measurements were taken at 1, 2 hours, 1 day, 4 days, 7 days, 14 days, and 30 days. This time range was chosen to determine the stability of the nanoparticles based on the change in maximum wavelength and the change in absorption value measured by UV-Vis spectrophotometer.

8. Preparation for the 1000 ppm Heavy Metal Solution

Cadmium, Copper, Lead, Manganese, Zinc, Mercury, Aluminum, Potassium, and Magnesium ion with concentration of 1000 ppm were soluble into 100 mL measuring cup with aquadest solvent and stored by using amber reagent bottles in 25℃ (room temperature). These metal ions were obtained from different salts compounds and with different amounts, including 0.0208 grams cadmium sulfate, 0.0134 grams copper(II) chloride, 0.0331 grams lead(II) nitrate, 0.0151 grams manganese sulfate, 0.0136 grams zinc chloride, 0.0325 grams mercury(II) nitrate, 0.0134 grams aluminum chloride, 0.0166 grams potassium iodide, and 0.00243 grams magnesium chloride.

9. Colorimetric Analysis with Silver Nanoparticles

Each analyte solution containing Cd^{2+}, Cu^{2+}, Pb^{2+}, Mn^{2+}, Zn^{2+}, Al^{3+}, Hg^{2+}, K^{+}, Mg^{2+}, as much as 2 mL with a concentration of 1000 ppm is added with 1 mL of AgNPs. The test results are visually observed if the color change of the solution occurs (within <5 minutes), where if the color changes before 5 minutes then the time was recorded as the time the color change occurs. Then the solution was characterized with a UV-Vis spectrophotometer in the wavelength range of 300-800 nm.

10. Method Validation Test

The method validation test includes selectivity, interference tests, sensitivity, and linearity, as well as LOD and LOQ was carried out by measuring the absorbance of a mixture of nanoparticles with selected metal ions that underwent color change. As for this selectivity test, each metal ions were mixed with nanoparticles at a ratio of 1:2, which were 2 mL of nanoparticles coupled with 4 mL of selected metal ions with varying

concentrations of 100-1000 ppm. Selectivity was assessed by comparing the change of colour and absorbance intensity of the AgNPs for each metal ions. If only AgNPs with Hg^{2+} that had lower intensity or greater decrease in colour and absorbance, it is indicated higher selectivity of AgNPs as Hg^{2+} colorimetric sensor. Interference was assessed by measuring the absorbance of the AgNPs solution upon addition of a target metal ion in the presence of an equimolar amount of potential interfering metal ions. As for sensitivity and linearity was carried out by mixture synthesized AgNPs solution with selected metal ion for several concentration standards to make calibration curve. As for LOD and LOQ tests was carried out by measuring absorbance of the blank solution, which is aquadest. LOD and LOQ values were obtained from the slope's standard deviation (σ) in the linearity plot: LOD is 3.3 σ/slope, while LOQ is 10 σ/slope. That several tests was characterized by using a spectrophotometer to calculate the wavelength in the lambda range of 200-800 nm. That several tests was characterized by using a spectrophotometer to calculate the wavelength in the lambda range of 200-800 nm.

11. Data Analysis

After obtaining the calibration curve for the sensitivity and linearity results, the next step was regression analysis for linearity. From the curve, the equation of the line was obtained with the value of y = mx+c where m = slope and c = intercept.

RESULTS AND DISCUSSION

1. GCMS Tests of Ethyl Acetate Fraction of Lemongrass Leaves

Figure 1. Photograph of ethyl acetate fraction

Figure 1 shows the appearance of the ethyl acetate fraction with a concentration fractinated extract of 15.7%, confirming successful separation. Testing with GCMS is carried out to confirm the presence of these compounds to support the data from the phytochemical test results. The table of GCMS chromatogram results is in Table 1**.** The results of the Gas Chromatography Mass Spectrophotometer analysis of kitchen lemongrass leaves showed that there were 10 compounds that constituted lemongrass leaves which were a group of ester compounds (2-Propenoic acid, 3-(4-hydroxy-3-methoxyphenyl)-,methyl ester; Hexadecanoic acid, methyl ester; 9,12,15-Octadecatrienoic acid, methyl ester), carboxylic acids (Docosanoic acid, methyl ester), terpenoids (Neophytadien), triterpenoids (DA-Friedoursan 3-one), ketones (Isophorone), and aldehydes (6-Methyl-4,6-bis(4-methylpent-3-en-1-yl) 1,3-dienecarbaldehyde). However, compounds that dominate in the fraction including DA-Friedoursan 3-one, 6-Methyl-4,6-bis(4-

methylpent-3-en-1-yl) 1,3-dienecarbaldehyde, Isophorone, and 2-Propenoic acid, 3-(4-hydroxy-3-methoxyphenyl)-,methyl ester.

Table 1 shows that ester compounds exhibit longer retention times compared to other compounds (e.g., Isophorone in 6.397 meanwhile Hexadecanoic acid methyl ester in 30.806). This because the boiling point of the ester compound is relatively high, so it will 'elute later due to higher boiling points, and the signal captured by the detector will be longer than other compounds. According to the research of [11] there are 13 constituent compounds and 3 major compounds produced are Citronellal, Citronellol, Geraniol which are characteristic of essential oil compounds, namely the monoterpenoid group. According to the research of [15] method produced 33 constituent compounds, including monoterpenoids and sesquiterpenes. There are 3 monoterpene compounds that are dominant in the composition of essential oils, namely 1-β-pinen, Z-citral, and E-citral. From some of these studies, there are quite a lot of significant differences in organic compounds produced This is because in this study, extraction is carried out gradually by fractionating the liquid-liquid extraction method, and due to differences in the use of solvents or conditions during the extraction of lemongrass leaves [11].

Table 1. Compounds identified in the ethyl acetate fraction of lemongrass leaves by GC-MS

Sample	RT	Quality	Compound	Content (%)
Ethyl Acetate Fraction Extract	41.535	89	DA-Friedoursan 3-one	6.77
	32.22	99	6-Methyl-4,6-bis(4-methylpent-3-en-1-yl) 1,3-dienecarbaldehyde	4.4
	6.397	94	Isophorone	3.7
	30.247	97	2-Propenoic acid, 3-(4-hydroxy-3-methoxyphenyl)-,methyl ester	3.24
	29.779	96	Neophytadien	2.85
	30.806	99	Hexadecanoic acid, methyl ester	2.71
	32.123	99	9,12,15-Octadecatrienoic acid, methyl ester	2
	32.626	94	1-Docosene	1.88
	32.275	95	Methyl sterarate	1.59
	34.92	92	Docosanoic acid, methyl ester	1.52

4. Nanoparticles Synthesis

Based on Figure 2, reddish-brown colloidal silver nanoparticles have been successfully synthesized. Visual color changes that can be observed organoleptic are caused by the resonance effect that occurs between energy and matter, nanoparticles that have successfully undergone formation due to the nucleation effect [16].

Reductor agents play an essential role in AgNP synthesis because they drive the reduction of Ag^+ ions into metallic silver that subsequently forms AgNPs. Functional groups in organic compounds, particularly those containing O, H, S, and N, are critical

in sustaining the nucleation stage in the AgNP formation mechanism [13]. Identification of the active functional groups therefore provides an important basis for explaining the progression of nanoparticle formation and stability.

Figure 3 illustrates that ester hydrolysis can generate carboxylic acid compounds as reaction products. Silver nitrate ($AgNO_3$) releases Ag^+ cations, which are reduced through interaction with reactive ligands, notably hydroxyl groups (OH^-). Hydroxyl groups arise from the hydrolysis of ester rich compounds that are predominantly present in lemongrass leaf extract after fractionation using ethyl acetate via liquid liquid extraction. Reaction conditions at alkaline pH 10 accelerate hydroxyl availability and increase reactivity due to stronger nucleophilicity in the system.

Figure 2. Colloidal silver nanoparticles

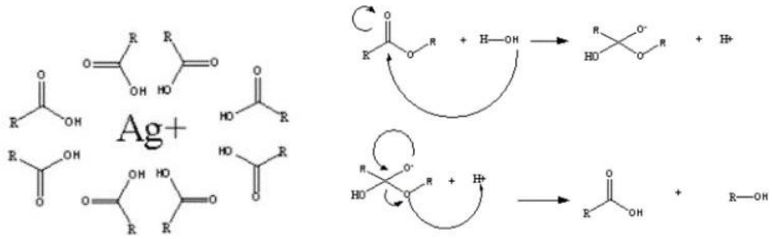

Figure 3. Ester hydrolysis reaction mechanism

Alkaline conditions promote electron density and facilitate bond cleavage, resulting in a more reactive leaving group. Electron attack by hydroxyl species on the tertiary carbon can generate a carbanion intermediate, followed by destabilization of the carbonyl bonding system after nucleophilic addition. Elimination steps then occur because oxygen containing intermediates with excess electron density are unstable and tend to seek proton stabilization, leading to repeated bond cleavage and formation of carboxylic acid compounds as stable products.

Hydroxyl groups produced during ester hydrolysis also contribute to the nucleation process by coordinating with Ag^+ precursors. Electron sharing between Ag^+ and hydroxyl ligands promotes coordinated covalent interactions that support early nucleus formation. Hydroxyl ligands can form an electrostatic or electromagnetic protective

layer on the nucleus surface, limiting agglomeration and improving nanoparticle stability. Compounds that act simultaneously as reducers and stabilizers are known as capping agents, and effective capping agents help maintain small particle size by preventing uncontrolled aggregation during growth [13], [17].

A nucleation mechanism is required in AgNP synthesis to enable interactions between the precursor agent and its ligand through coordinated covalent bonding. This causes the energy absorbed by an atom to form a higher energy level as a result of more chromophore groups being formed. Based on Figure 4a-d, which is the SPR of each optimization method of nanoparticle synthesis.The concentration of the extract used as much as 10% has the highest absorbance value and the maximum wavelength that is hypsochromic (blue shift) is 416 nm. The wavelength produced corresponds to the wavelength of the nanoparticle wavelength, which is 400-450 nm, meaning that silver nanoparticles have been formed [18].

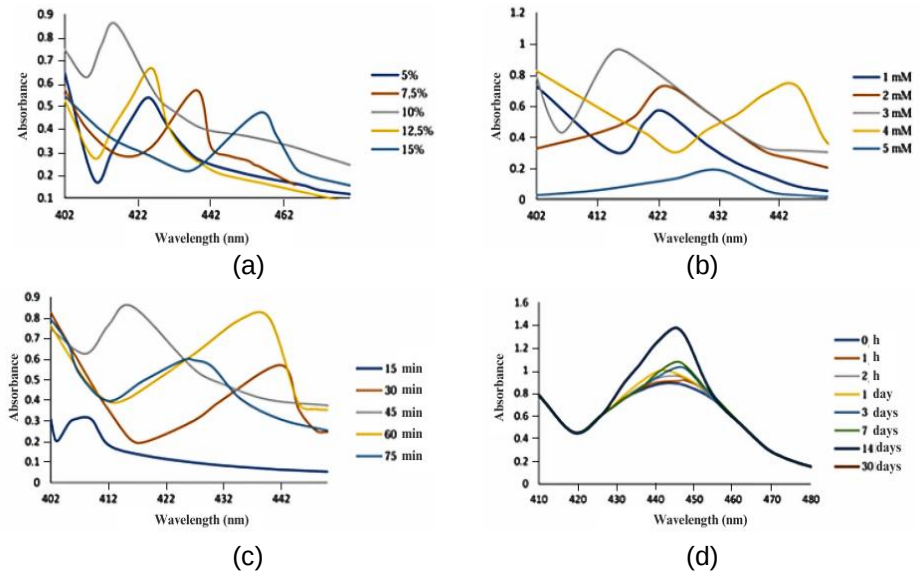

Figure 4a-d. Optimization of AgNPs synthesis with parameters of (a) extract concentration, (b) $AgNO_3$ concentration, (c) reaction time and (d) nanoparticle stability over 30 days

The concentration of $AgNO_3$ used as much as 3 mM has the highest absorbance value and the maximum hypsochromic wavelength (blue shift) is 416 nm. The wavelength produced corresponds to the wavelength of the nanoparticle wavelength, which is 400-450 nm, meaning that AgNPs have been formed. This happens because the higher the concentration of $AgNO_3$ used, which in this case acts as a precursor agent of the coordination covalent binding reaction, the concentration increases, so that the absorbance value produced will also increase. However, at a certain concentration level, absorbance will experience a reversal of decline because the energy level produced by the hydrogen bond formed between the water solvent and its chromophore group is saturated, so that the nanoparticles formed are increasingly agglomerated due to

excessive nucleation reactions. This affects the size of the nanoparticles that get bigger and bigger and reshape into their bulky particles [19].

The synthesis reaction time of 45 minutes has the highest absorbance value of 0.856 and the maximum hypsochromic wavelength (blue shift) of 416 nm. The wavelength produced corresponds to the wavelength of the nanoparticle wavelength, which is 400-450 nm, meaning that AgNPs have been formed. The duration of synthesis time between the precursor agent and its ligands that form nanoparticles greatly affects the quantity of nanoparticles produced. The longer the duration of the collision between the particles that occurs, the more nanoparticles are formed, so that more silver nanoparticles agglomerate and have the effect of producing large nanoparticle sizes. Based on the instability of nanoparticle formation, the reaction time factor is one of the important things, therefore, it needs the optimum reaction time needed to produce a better shape and size of nanoparticles [19].

AgNPs stored under optimum synthesis conditions without further heating showed acceptable stability because absorbance over 30 days increased only gradually. This pattern indicates that heating during synthesis strongly influences nanoparticle formation, since ligand molecules responsible for reducing Ag^+ can remain active even after heating is stopped. Continued activity of reducing functional groups can promote ongoing nanoparticle growth during storage, which gradually increases particle size through agglomeration and can reduce stability over time.

Silver nanoparticle formation proceeds through coordinated nucleation between the precursor and its ligand. Ligands that also act as capping agents can provide partial stabilization by forming an electrostatic or electromagnetic protective layer around Ag^0, which helps slow the formation rate and limits uncontrolled growth [20]. Limited long term stability can occur because no additional stabilizing agent is introduced, allowing agglomeration to proceed as nucleation and growth continue, ultimately favoring the formation of larger particles or nanoclusters that accelerate aggregation processes [20].

5. Nanoparticles Characterization

FTIR characterization was conducted to identify functional group bonds that potentially act as bioreductors during AgNP synthesis. Figure 5a presents the infrared spectrum of the ethyl acetate extract. An absorption band at 2984 cm^{-1} indicates the presence of C H sp^3 vibrations, while a peak at 1736 cm^{-1} corresponds to carbonyl (C=O) stretching typically associated with ester functional groups. A band at 1447.21 cm^{-1} suggests aliphatic C H vibrations, and an absorption feature around 1233.76 cm^{-1} reflects C O C vibrations that may be linked to polysaccharides or complex carbohydrates. These signals support the presence of ester containing constituents in the ethyl acetate fraction.

Figure 5b shows the infrared spectrum obtained after AgNP synthesis. A broad band at 3331.28 cm^{-1} indicates O H stretching, suggesting hydroxyl groups associated with

the capped nanoparticle surface or reaction products. A peak at 1637.74 cm^{-1} indicates possible carbonyl (C=O) stretching consistent with carboxylic acid formation. Bands observed at 2087 cm^{-1} and 2353 cm^{-1} indicate the presence of conjugated functional group vibrations, supporting structural changes after reduction and nanoparticle formation. These spectral shifts provide evidence that AgNPs were formed, accompanied by chemical transformations that are consistent with ester hydrolysis and the reduction of Ag^{+} to Ag^{0}.

Several absorption bands detected in the original extract were absent after synthesis, indicating the consumption or transformation of certain functional groups during the reaction. Loss of bands associated with aliphatic structures and complex carbohydrate related vibrations can be explained by hydrolysis and elimination steps that stabilize reaction intermediates and generate new carbonyl containing products. Hydroxyl group formation is consistent with ester hydrolysis in alkaline conditions, where nucleophilic attack by water derived O H species proceeds rapidly and contributes to both reduction and stabilization processes [21].

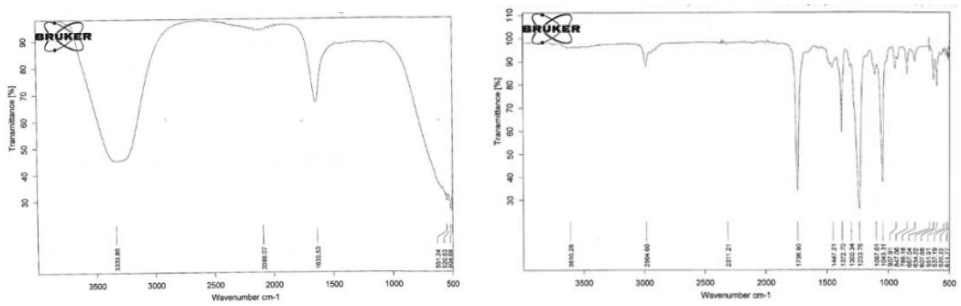

(a) (b)

Figure 5. (FTIR result of (a) ethyl acetate extract (b) AgNPs

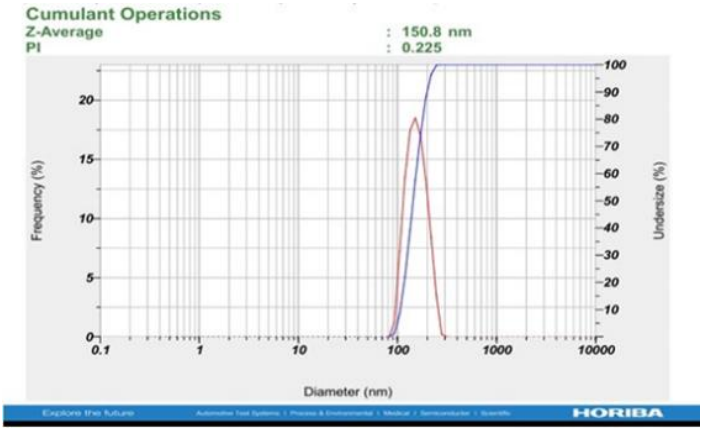

Figure 6. Results of particle distribution with PSA on nanoparticles

Characterization with PSA or particle size analyzer aims to determine the particle size distribution using dynamic light scattering. DLS uses light scattering effects and Brown's motion changes to estimate particle size distributions [21]. Based on Figure 6, it can be seen that the average diameter size of the nanoparticles produced

from lemongrass leaf extract is 150.8 nm with a polydispersity index (PI) of 0.225 and a single diameter size of 34.9 nm and a count rate of 1107 kCPS. Previous research showed that AgNPs synthesized from lemongrass leaf extract had particle sizes of 13.1–30.9 nm [22]. From the results and data of previous research, it can be concluded that the AgNPs that synthesized from this study has a larger size than previous research. Ideally, nanoparticles should have a size of 10-100 nm. Nanoparticles with a size greater than 100 nm indicate that agglomeration has occurred in the nanoparticles [23]. The aggregation or size of AgNPs can affect sensor performance, one of which is the sensitivity parameter. The larger the AgNPs, the smaller the surface area, so the less area of analyte binding is detected. However, larger AgNPs sometimes has a larger visible color shift, which makes them more effective as sensors [24].

Bioreductors can act as capping agents that can maintain the stability of nanoparticles to be able to agglomerate, but if the stabilization effect is not optimal, the Coulomb force or rejection of the nanoparticles will also be smaller, as a result the Zeta Potential value will also be smaller, or even non-existent. This will cause the nanoparticles to agglomerate more easily and form a much larger diameter of size. If the polydispersity index is in the range of monodisperse form, and the count rate has a high speed, it turns out that the diameter of the resulting nanoparticles is relatively large. This is because the average particle distribution has undergone agglomeration and causes colloidal nanoparticles to flocculate, so that the distribution is uneven, and causes the size of the detected nanoparticles to increase as a whole [25], [26].

6. Method Validation and Data Analysis

Figure 7 shows the visual color changes observed for each metal ion analyte after the addition of AgNPs. A pronounced response was observed for mercury ions (Hg^{2+}), where the solution gradually became clear. This phenomenon indicates a strong interaction between Hg^{2+} and AgNPs that alters the optical properties of the nanoparticle system.

The color disappearance is attributed to a spontaneous redox reaction between AgNPs and Hg^{2+}, driven by a substantial difference in cell potential between the two species [21]. Redox driven transformation can disrupt the nanoparticle surface and modify the surface plasmon resonance behavior, leading to a loss of the characteristic color associated with AgNP colloids. Evidence of this selective response aligns with the concept that AgNPs prepared using different bioreductors may exhibit distinct surface chemistries and reactivity profiles.

Variation in selectivity is also influenced by differences in ligand characteristics on the AgNP surface. Carboxylic acid derived ligands can differ in polarity index and electron affinity, affecting electronegativity distribution and coordination behavior. Differences in ligand properties may promote stronger coordinated covalent interactions between AgNP bound ligands and Hg^{2+} compared with other cations,

resulting in the formation of stable complexes that can even outperform interactions with the original precursor Ag^+ [27]. SPR measurements using a UV Vis spectrophotometer were conducted to support these observations, as presented in Figure 8a.

Figure 9 and Figure 8b indicate that at a Hg^{2+} concentration of 600 ppm, the absorbance peak no longer appeared within the typical AgNP SPR region. Peak shifting toward 642 nm was observed, which is associated with oxidized metal ion related absorption. This shift suggests that extensive aggregation or transformation occurred, likely because coordinated interactions and redox processes promoted nanoparticle agglomeration into larger particles that no longer exhibit the standard nanoparticle SPR response [28].

Figure 7.Colorimetric detection with severe heavy metals

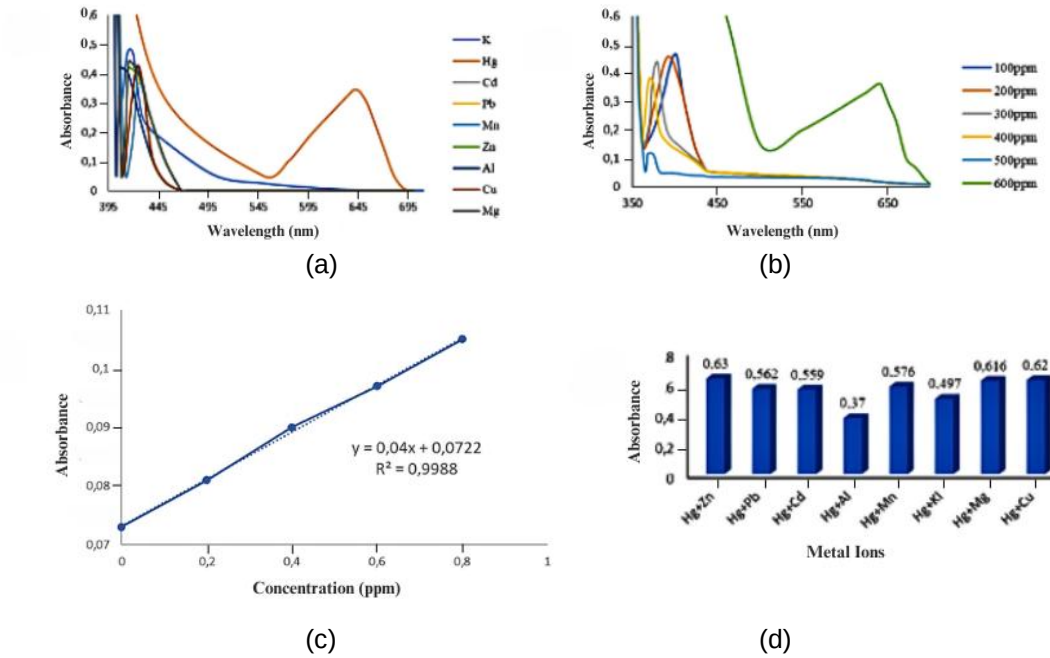

Figure 8. (a) Colorimetric spectral results of several metals, (b) Results of selectivity method validation test, (c) Linear regression curve, (d) Heavy metal interference test

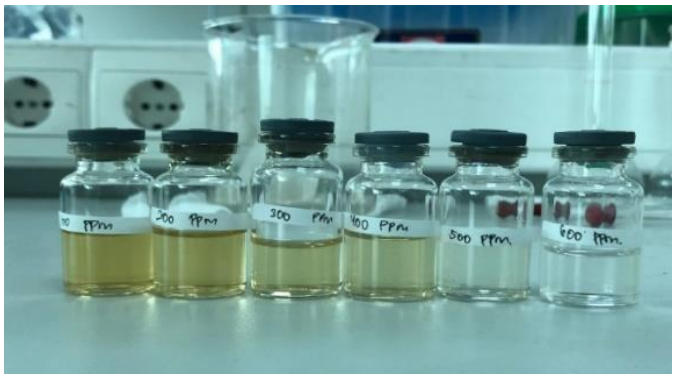

Figure 9. Selectivity with mercury ion using organoleptic methods

Interference testing presented in Figure 8d showed that Zn^{2+}, Mg^{2+}, and Cu^{2+} produced the highest interference toward Hg^{2+} detection. Limited ability of these cations to form stable coordinated complexes with AgNPs can leave AgNPs in their nanoparticle state, thereby reducing the efficiency of Hg^{2+} induced oxidation and complex formation. Similarities in cell potential among Zn^{2+}, Mg^{2+}, and Cu^{2+} can also allow redox reactions to occur but with weaker spontaneity, contributing to competitive effects that suppress Hg AgNP formation and decrease detection efficiency [29].

Figure 8c, showed the regression value R^2 = 0.9988 with the value of y = mx+c where m = slope and c = intercept. The requirement for the value of the correlation coefficient (R^2) is >0.995. Based on the regression curve results obtained, it is said that the AgNPs method as a mercury metal colorimetric sensor is valid and acceptable. In the figure above, it shows the value of linearity with the regression equation y = 0.04x + 0.0722. Where the equation has a slope value of 0.04. Based on calculations with the Lambert-Beer law [30], a sensitivity value of 10.84 × 10^3 L mol^{-1} cm^{-1} was obtained. In this study, a method of determining the blank solution was used. The results of the calculation of LOD and LOQ values are 3.681× 10^{-6} ppb and 1.115 × 10^{-5} ppb. This result is obtained from the LOD formula equation, which is 3.3 SD/slope, and LOQ 10 SD/slope [31]. The standard deviation was obtained from 10x repeats of the absorption of the blank solution at a wavelength of 432 nm

CONCLUSION

Nanoparticles synthesized using lemongrass leaf extract (*Cymbopogon citratus*) under alkaline conditions reached optimum formation at 45 minutes with $AgNO_3$ concentration of 3 mM, extract concentration of 10%, and pH 10. The resulting AgNPs formed a reddish brown colloid with an SPR peak at 432 nm and an average diameter of 150.8 nm measured by DLS. Selective colorimetric response toward Hg^{2+} highlights the relevance of this sensor system given the environmental toxicity of mercury.

Sensor performance indicated strong analytical capability, with Hg^{2+} selectivity observed up to 600 ppm, a molar absorptivity of 10.84 × 10^3 L mol^{-1} cm^{-1}, excellent linearity (R^2 = 0.9988), and high sensitivity reflected by LOD of 3.681 × 10^{-9} ppm and LOQ of

1.115 × 10^{-8} ppm. Future work should prioritize real sample validation and development of practical formats such as thin films or paper based sensors for field use. A limitation of this study lies in the relatively large particle size above 100 nm, suggesting aggregation, yet the green synthesis approach remains important because it avoids harmful reagents while supporting safer mercury detection in water.

ACKNOWLEDGEMENT

The authors would like to thank the Rector and Head of LPPM UNJ who have facilitated this research by providing grant funds for the faculty basic with a Contract Agreement Letter Number: 16/SPK PENELITIAN/5.FMIPA/2025.

REFERENCES

[1] Kementerian Lingkungan Hidup dan Kehutanan, "Peraturan Pemerintah Republik Indonesia No. 22 Tahun 2021 tentang Penyelenggaraan Perlindungan dan Pengelolaan Lingkungan Hidup." Sekretariat Negara, Jakarta, 2021.

[2] W. C. Nugraha, Y. Ishibashi, and K. Arizono, "Assessment of heavy metal distribution and contamination in the sediment of the Ciujung Watershed, Banten Province, Indonesia," *J Mater Cycles Waste Manag*, vol. 25, no. 5, pp. 2619–2631, Sep. 2023, doi: 10.1007/s10163-023-01661-4

[3] A. Khatoon, J. A. Syed, A. R. Solangi, A. Mallah, and Sirajuddin, "Mechanistic insights of mercury ion detection and its influence on time monitored hydrodynamic size of Capsicum Annumm C derived silver nanoparticles during colorimetric nano-sensing," *Optik (Stuttg)*, vol. 325, p. 172237, Apr. 2025 (Early Access), doi: 10.1016/j.ijleo.2025.172237

[4] S. Kokilavani *et al.*, "Highly selective and sensitive tool for the detection of Hg(II) using 3-(Trimethoxysilyl) propyl methacrylate functionalized Ag-Ce nanocomposite from real water sample," *Spectrochim Acta A Mol Biomol Spectrosc*, vol. 242, p. 118738, Dec. 2020, doi: 10.1016/j.saa.2020.118738

[5] G. Ghodake *et al.*, "Gallic acid-functionalized silver nanoparticles as colorimetric and spectrophotometric probe for detection of Al3+ in aqueous medium," *Journal of Industrial and Engineering Chemistry*, vol. 82, pp. 243–253, Feb. 2020, doi: 10.1016/j.jiec.2019.10.019

[6] Y. Wang *et al.*, "Facile and Green Fabrication of Carrageenan-Silver Nanoparticles for Colorimetric Determination of Cu2+ and S2−," *Nanomaterials*, vol. 10, no. 1, p. 83, Jan. 2020, doi: 10.3390/nano10010083

[7] G. Franci *et al.*, "Silver Nanoparticles as Potential Antibacterial Agents," *Molecules*, vol. 20, no. 5, pp. 8856–8874, May 2015, doi: 10.3390/molecules20058856

[8] J. Hernandez-Sandoval, G. H. Garza-Elizondo, A. M. Samuel, S. Valtiierra, and F. H. Samuel, "The ambient and high temperature deformation behavior of Al–Si–Cu–Mg alloy with minor Ti, Zr, Ni additions," *Mater Des*, vol. 58, pp. 89–101, Jun. 2014, doi: 10.1016/j.matdes.2014.01.041

[9] A. L. Yulifianti, B. Eristi, M. Puspita, and D. Handayani, "Process Engineering Communication Media and Appropriate Technology for Ginger Pulp Filtration Using Filter Press," *METANA*, vol. 15, no. 2, pp. 43–48, Nov. 2019, doi: 10.14710/metana.v15i2.25086

[10] A. Rautela, J. Rani, and M. Debnath (Das), "Green synthesis of silver nanoparticles from Tectona grandis seeds extract: characterization and mechanism of antimicrobial action on different microorganisms," *J Anal Sci Technol*, vol. 10, no. 1, p. 5, Dec. 2019, doi: 10.1186/s40543-018-0163-z

[11] R. A. Syarif, F. Faradiba, A. Tenri, M. Khaira, and N. Nirwana, "GC-MS Analysis of Lemongrass with Various Extraction Methods," *Jurnal Fitofarmaka Indonesia*, vol. 10, no. 3, pp. 1–6, 2023, doi: 10.33096/jffi.v10i3.1108

[12] L. U. Khasanah, S. Ariviani, E. Purwanto, and D. Praseptiangga, "Chemical composition and citral content of essential oil of lemongrass (Cymbopogon citratus (DC.) Stapf) leaf waste prepared with various production methods," *J Agric Food Res*, vol. 19, p. 101570, Mar. 2025 (Early Access), doi: 10.1016/j.jafr.2024.101570

[13] S. J. Nadaf *et al.*, "Green synthesis of gold and silver nanoparticles: Updates on research, patents, and future prospects," *OpenNano*, vol. 8, p. 100076, Nov. 2022, doi: 10.1016/j.onano.2022.100076

[14] S. N. Nacer *et al.*, "Phytochemical screening, antioxidant, antibacterial, and antifungal properties of the Cymbopogon citratus methanolic extract," *Pharmacological Research - Natural Products*, vol. 5, p. 100094, Dec. 2024 (Early Access), doi: 10.1016/j.prenap.2024.100094

[15] N. I. Anggraeni, I. W. Hidayat, S. D. Rachman, and Ersanda, "Bioactivity of essential oil from lemongrass (*Cymbopogon citratus* Stapf) as antioxidant agent," *AIP Conference Proceedings*, vol. 1927, no. 1, Art. no. 030007, Feb. 2018. [Online]. Available: doi: 10.1063/1.5021200

[16] R. Suárez-López, V. F. Puntes, N. G. Bastús, C. Hervés, and C. Jaime, "Nucleation and growth of gold nanoparticles in the presence of different surfactants. A dissipative particle dynamics study," *Sci Rep*, vol. 12, no. 1, p. 13926, Aug. 2022, doi: 10.1038/s41598-022-18155-2

[17] S. Islam, S. Bairagi, and M. R. Kamali, "Review on green biomass-synthesized metallic nanoparticles and composites and their photocatalytic water purification applications: Progress and perspectives," *Chemical Engineering Journal Advances*, vol. 14, p. 100460, May 2023, doi: 10.1016/j.ceja.2023.100460

[18] A. M. Sivalingam and A. Pandian, "Characterization of silver nanoparticles (AgNPs) synthesized using polyphenolic compounds from Phyllanthus emblica L. and their impact on cytotoxicity in human cell lines," *Carbohydrate Polymer Technologies and Applications*, vol. 8, p. 100535, Dec. 2024, doi: 10.1016/j.carpta.2024.100535

[19] Y. Pratiwi, Y. Yusmaniar, and N. Nurhasanah, "Biosynthesis of Poly Acrylic Acid (PAA) Modified Silver Nanoparticles, Using Basil Leaf Extract (Ocimum basilicum L.) for Heavy Metal Detection," *JKPK (Jurnal Kimia dan Pendidikan Kimia)*, vol. 8, no. 3, p. 323, Dec. 2023, doi: 10.20961/jkpk.v8i3.78641

[20] Y. Pratiwi, A. Widyaresti, T. Hadinugrahaningsih, E. V. Nanda, and D. N. Anisa, "Synthesis of Poly Acrylic Acid (PAA) Modified Silver Nanoparticles, Using Trisodium Citrate for Heavy Metal Detection," *JKPK (Jurnal Kimia dan Pendidikan Kimia)*, vol. 9, no. 3, pp. 514–533, Dec. 2024, doi: 10.20961/jkpk.v9i3.91340

[21] P. Dhanyasree, K. V. Neenu, D. Anna David, P. M. Sabura Begum, and K. Yoosaf, "An eco-friendly Polymer-Silver nanocomposite film for simultaneous sensing and removal of mercury from water," *Microchemical Journal*, vol. 207, p. 112188, Dec. 2024 (Early Access), doi: 10.1016/j.microc.2024.112188

[22] A. Tazi, A. Zinedine, J. M. Rocha, and F. Errachidi, "Review on the pharmacological properties of lemongrass (Cymbopogon citratus) as a promising source of bioactive compounds," *Pharmacological Research - Natural Products*, vol. 3, p. 100046, Jun. 2024, doi: 10.1016/j.prenap.2024.100046

[23] P. Bélteky *et al.*, "Are Smaller Nanoparticles Always Better? Understanding the Biological Effect of Size-Dependent Silver Nanoparticle Aggregation Under Biorelevant Conditions," *Int J Nanomedicine*, vol.

Volume 16, pp. 3021–3040, Apr. 2021, doi: 10.2147/IJN.S304138

[24] J. Dolai, K. Mandal, and N. R. Jana, "Nanoparticle Size Effects in Biomedical Applications," *ACS Appl Nano Mater*, vol. 4, no. 7, pp. 6471–6496, Jul. 2021, doi: 10.1021/acsanm.1c00987

[25] A. Singh, V. A. Chavan, P. Ariya, B. Udaynadh, and E. Adithi, "Nanomaterial Characterization Techniques," in *Futuristic Trends in Chemical Material Sciences & Nano Technology Volume 3 Book 13*, Iterative International Publishers, Selfypage Developers Pvt Ltd, 2024, pp. 18–45. doi: 10.58532/V3BECS13P1CH2

[26] C. Tyavambiza, A. M. Elbagory, A. M. Madiehe, M. Meyer, and S. Meyer, "The Antimicrobial and Anti-Inflammatory Effects of Silver Nanoparticles Synthesised from Cotyledon orbiculata Aqueous Extract," *Nanomaterials*, vol. 11, no. 5, p. 1343, May 2021, doi: 10.3390/nano11051343

[27] Y. Zhang, S. Prabakar, and E. C. Le Ru, "Coadsorbed Species with Halide Ligands on Silver Nanoparticles with Different Binding Affinities," *The Journal of Physical Chemistry C*, vol. 126, no. 20, pp. 8692–8702, May 2022, doi: 10.1021/acs.jpcc.2c01092

[28] S. Kasim, P. Taba, Ruslan, and R. Anto, "Sintesis Nanopartikel Perak Menggunakan Ekstrak Daun Eceng Gondok (Eichornia crassipes) Sebagai Bioreduktor," *KOVALEN: Jurnal Riset Kimia*, vol. 6, no. 2, pp. 126–133, Sep. 2020, doi: 10.22487/kovalen.2020.v6.i2.15137

[29] N. Riveli, "Dynamic Light Scattering Simulation to Investigate the Effect of Wavelength on Particle Size Measurement Accuracy," *Jurnal Material dan Energi Indonesia*, vol. 13, no. 01, p. 39, Aug. 2023, doi: 10.24198/jme.v13i01.49188

[30] N. N. Trisnawati, I. G. A. K. S. P. Dewi, P. P. V Suari, and N. P. A. Krismayanti, "Validation of Metode Mercury Test using Inductively Coupled Plasma Emission Spectrometry (ICPE) 9000," *Indonesian E-Journal of Applied Chemistry*, vol. 9, no. 1, pp. 24–28, Aug. 2021.

[31] A. Aminu and S. A. Oladepo, "Fast Orange Peel-Mediated Synthesis of Silver Nanoparticles and Use as Visual Colorimetric Sensor in the Selective Detection of Mercury(II) Ions," *Arab J Sci Eng*, vol. 46, no. 6, pp. 5477–5487, Jun. 2021, doi: 10.1007/s13369-020-05030-3